

Electronic Supplementary information

Insight into the Effect of Intercalated Alkaline Cations of Layered Manganese Oxides on Oxygen Reduction Reaction and Oxygen Evolution Reaction

Soracha Kosasang^a, Nattapol Ma^a, Phatsawit Wuamprakhon^a, Nutthaphon Phattharasupakun^a, Thana Maihom^{a,b,c}, Jumras Limtrakul^{a,c}, Montree Sawangphruk^{a,*}

^aDepartment of Chemical and Biomolecular Engineering, School of Energy Science and Engineering, Vidyasirimedhi Institute of Science and Technology, Rayong 21210, Thailand.

^b Department of Chemistry, Faculty of Liberal Arts and Science, Kasetsart University, Kamphaeng Saen Campus, Nakhon Pathom 73140, Thailand

^cLaboratory for Computational and Applied Chemistry, Department of Chemistry, Faculty of Science and Center for Advanced Studies in Nanotechnology and Its Applications in Chemical, Food and Agricultural Industries, Kasetsart University, Bangkok 10900, Thailand.

Laboratory for Computational and Applied Chemistry, Department of Chemistry, Faculty of Science and Center for Advanced Studies in Nanotechnology and Its Applications in Chemical, Food and Agricultural Industries, Kasetsart University, Bangkok 10900, Thailand.

*Corresponding author. Tel: +66(0)33-01-4251 Fax: + 66(0)33-01-4445.

E-mail address: montree.s@vistec.ac.th (M. Sawangphruk).

ORCID ID: <https://orcid.org/0000-0003-2769-4172>

Experimental section

Chemicals and Materials

Manganese(II) nitrate tetrahydrate ($\text{Mn}(\text{NO}_3)_2 \cdot 4\text{H}_2\text{O}$, 98%, Loba Chemie), lithium hydroxide (LiOH, 98%, Sigma-Aldrich), sodium hydroxide (NaOH, 99.8%, Ajax Finechem), potassium hydroxide (KOH, Ajax Finechem), Rubidium hydroxide (RbOH, 50%, Sigma-Aldrich), Cesium hydroxide (CsOH, 50%, Sigma-Aldrich), hydrogen peroxide (H_2O_2 , 30%, Chem Merck), Polyvinylidene fluoride (PVDF, $M_w \sim 534,000$, Sigma-Aldrich), carbon black (TIMCAL), N-Methyl-2-pyrrolidone (NMP, 99.5%, Qrec), ruthenium chloride trihydrate ($\text{RuCl}_3 \cdot 3\text{H}_2\text{O}$, Sigma-Aldrich), and methanol (MeOH, 99.5%, Sigma-Aldrich) are analytical grade and used without further purification. Carbon fiber paper (CFP, SGL CARBON SE, Germany) was used as substrate. Deionized water was purified by using Milli-Q system (DI water, 15 M Ω .cm, Millipore).

Synthesis of birnessite-type layered manganese oxides

Birnessite-type layered manganese oxide with lithium ion as an intercalated cation (Li-MnO_x) was prepared directly by adding a 100 mL solution of 1 M H_2O_2 and 0.6 M of $\text{LiOH} \cdot \text{H}_2\text{O}$ into 60 mL of 0.25 M $\text{Mn}(\text{NO}_3)_2 \cdot 4\text{H}_2\text{O}$ solution and stirring at room temperature for 1 h¹. The dark brown precipitate was observed, then filtered, washed with DI water, and dried at 50 °C for 2 days. Na-MnO_x , K-MnO_x , Rb-MnO_x , and Cs-MnO_x were prepared by the same procedure, except; NaOH, KOH, RbOH or CsOH was added, instead of adding $\text{LiOH} \cdot \text{H}_2\text{O}$, respectively^{2,3}.

Synthesis of RuO_2 nanoparticle

For the preparation of RuO_2 nanoparticles, 2 mmol of $\text{RuCl}_3 \cdot 3\text{H}_2\text{O}$ was dissolved in a mixture solution of DI water (20 ml) and MeOH (20 ml). The solution was stirred at room temperature. After stirred for 30 min, 2 M of NaOH was dropped into the stirred solution until the pH reached 7.0 and continuous stirring for 30 min. The obtained product was collected by centrifugation and washed with DI water in several times. Finally, the product was dried at 60 °C and then annealed at 500 °C with a heating rate of 1 °C/min for 2 h in air⁴.

Preparation of catalyst inks

Catalyst inks were prepared by dissolving the MnO_x with carbon black (CB) and polyvinylidene fluoride (PVDF) in a ratio of 7:1:2 d in N-Methyl-2-pyrrolidone (NMP) and sonicated for 2 hours. The catalyst inks then were dropped on a glassy carbon rotating electrode or on a carbon fiber paper (CFP).

Morphology and structure characterizations

The morphologies of as-synthesized samples were investigated by Field-emission scanning electron microscopy (FE-SEM, JSM-7001F, JEOL Ltd.) and Transmission electron microscopy (TEM, Hitachi operated at 120 kV). The crystallographic structures were characterized by powder x-ray diffraction (PXRD, Bruker D8 ADVANCE) using Cu K α radiation (30 kV, 40 mA) with a step size of 0.01° in the 2 θ range of 5-80°. Raman spectroscopy (Senterra Dispersive Raman, Bruker Optics, Germany, operated at a laser wavelength of 532 nm) were performed to identify the chemical structure of the samples. In situ Mn K-edge fluorescent X-ray absorption spectroscopy (XAS) was performed at Synchrotron Light Research Institute BL. 5.2 (Public Organization), Thailand. Note, XAS was equipped with Ge (220) double-crystal monochromator (energy range 3440-12100 eV).

Electrochemical characterization

A three-electrode configuration was used. The working electrode was a glassy carbon rotating disk electrode (RDE) with a diameter of 3 mm. A platinum rod and saturated calomel electrode (SCE) were used as the counter electrode and reference electrode, respectively. 2 μ L of catalyst ink was dropped on the RDE and dried at room temperature to make a thin film on the RDE. The catalytic activities on oxygen reduction reaction (ORR) and oxygen evolution reaction (OER) of the catalyst films were observed from the cyclic voltammograms (CV) and linear sweep voltammograms (LSV). The CV were performed in a potential range between 0 V and 2.3 V (V versus RHE) at a scan rate of 100 mV s⁻¹ under Ar or O₂ saturated in KOH solution (purging Ar or O₂ gas at least 40 min before the measurement). The LSV were recorded at a scan rate of 10 mV s⁻¹ under O₂ saturated in KOH solution at a different rotation rate. The catalyst ink (0.3 mg cm⁻²) was also loaded on the carbon fiber paper (CFP) to measure the catalytic activity and stability on the ORR and OER of the catalysts. The stability was measured by chronoamperometric technique at a constant potential of 0.7 V versus RHE. Metrohm AUTOLAB potentiostat (PGSTAT302N) was used to measure the electrocatalytic properties of all samples.

Calculation of electron transfer number (n) per oxygen molecule

Based on RDE data, the electron transfer number (n) per oxygen molecule can be determined by Koutechy-Levich (K-L) equation⁴⁻⁶.

$$\frac{1}{j} = \frac{1}{j_k} + \frac{1}{B\omega^{1/2}} \quad (S1)$$

j: current density (A cm⁻²)

j_k: kinetic current density (A cm⁻²)

ω : electrode rotating rate

B is determined from the slope of K-L plot according to Levich equation as given below:

$$B = 0.62nFD_{O_2}^{2/3}\nu^{-1/6}C_{O_2} \quad ; \text{ For } \omega \text{ in unit of rad s}^{-1} \quad (\text{S2})$$

or

$$B = 0.2nFD_{O_2}^{2/3}\nu^{-1/6}C_{O_2} \quad ; \text{ For } \omega \text{ in unit of rpm} \quad (\text{S3})$$

n represents for electron transfer number per oxygen molecule.

F is Faraday constant; 96485 C mol⁻¹

D_{O_2} is diffusion coefficient of O₂ in 0.1 M KOH solution (1.93 x 10⁻⁵ cm² s⁻¹)⁴⁻⁶.

ν is kinematic viscosity of the electrolyte, 0.1 M KOH solution (1.09 x 10⁻² cm² s⁻¹)⁴⁻⁶.

C_{O_2} is O₂-saturated concentration in 0.1 M KOH solution (1.26 x 10⁻⁶ mol cm⁻³)⁴⁻⁶.

In situ electrochemical X-ray absorption spectroscopy

In situ Mn K-edge XAS measurement was performed to examine the oxidation state of Mn under certain applied potential via chronoamperometry technique. In this measurement, a 3-electrode set up using the as-prepared catalysts on CFP as a working electrode, platinum wire as a counter electrode, SCE as a reference electrode in 0.1M KOH electrolyte. Note, the test cell with the dimension of 2 cm × 2 cm × 3.5 cm was fabricated from acrylic sheets with a square opening space on one of the 2-cm² sides (covered by a Kapton tape). Reference and counter electrodes were located alongside with the working electrode at ca. 1 cm (out of X-rays range). *In situ* measurement was performed at steady-state current by retaining the working electrode at a specific potential of interest for at least 15 min before the characterization.⁷⁻⁹

The oxidation state of Mn from XAS results was calculated using an empirical equation when located between Mn⁴⁺ and Mn³⁺ (S4), between Mn³⁺ and Mn^{2.67+} (S5), and between Mn^{2.67+} and Mn²⁺ (S6).¹⁰⁻¹²

$$\text{Oxidation state of Mn} = 4\left(\frac{\Delta E \text{ of sample}}{\Delta E \text{ of Mn}^{3+} \text{ and Mn}^{4+}}\right) + 3\left(1 - \frac{\Delta E \text{ of sample}}{\Delta E \text{ of Mn}^{3+} \text{ and Mn}^{4+}}\right) \quad (\text{S4})$$

$$\text{Oxidation state of Mn} = 3\left(\frac{\Delta E \text{ of sample}}{\Delta E \text{ of Mn}^{2.67+} \text{ and Mn}^{3+}}\right) + 2.67\left(1 - \frac{\Delta E \text{ of sample}}{\Delta E \text{ of Mn}^{2.67+} \text{ and Mn}^{3+}}\right) \quad (\text{S5})$$

$$\text{Oxidation state of Mn} = 2.67 \left(\frac{\Delta E \text{ of sample}}{\Delta E \text{ of Mn}^{2+} \text{ and Mn}^{2.67+}} \right) + 2 \left(1 - \frac{\Delta E \text{ of sample}}{\Delta E \text{ of Mn}^{2+} \text{ and Mn}^{2.67+}} \right) \quad (\text{S6})$$

Computational details

The surface models of a layer manganese oxide with the intercalated Li, Na, K, Rb, and Cs and water molecules are shown in Figure 4a, which were generated from their bulk structures from a slab cut along the (100) direction. A vacuum layer at least 20 Å was set between layers.

All calculations were performed within the Vienna Ab-initio Simulation Package (VASP) [1-2]. Projector augmented-wave (PAW) pseudopotentials were used to account for electron–ion interactions. The generalized gradient approximation (GGA) [3] with the Perdew–Burke–Ernzerhof (PBE) functional [4] was used to treat the exchange–correlation interaction between electrons. The long-range van der Waals interactions was described by using the empirical correction according to Grimme’s scheme (DFT-D2) [5]. To treat the localization of Mn 3d-electrons more accurately, an on-site Hubbard term U–J [6] of 4.0 eV [7] was applied. The energy cut off was set to 450 eV and 3 x 3 x 1 Monkhorst–Pack was used to sample the Brillouin zone. The convergence thresholds for full geometry optimizations were 10⁻⁵ eV and 0.005 eV/Å for total energy and ionic force, respectively.

Four-step mechanism reinforced by previous theoretical^{8,9} and experimental¹⁰ works was assumed to identify fundamental aspects of OER/ORR reaction process. The OER reaction can be occurred as following equations (the ORR is reverse reaction of the OER).



where * denotes an active site on layer MnO₂, and the *O₂, *OH, *O, and *OOH refer to the intermediates existing in electrocatalysts. The transformation step either from *OH to *O or the formation of *OOH from *O are able to be rate-determining step of the reactions as verified by the equations above. The absorption energies were calculated as follows:

$$\Delta E_{* \text{OH}} = E_{* \text{OH}} + 1/2 E_{\text{H}_2} - E_* - E_{\text{H}_2\text{O}} \quad (\text{S5})$$

$$\Delta E_{* \text{O}} = E_{* \text{O}} + E_{\text{H}_2} - E_* - E_{\text{H}_2\text{O}} \quad (\text{S6})$$

$$\Delta E_{*OOH} = E_{*OOH} + 3/2E_{H_2} - E_* - 2E_{H_2O} \quad (S7)$$

where, E_* is the energy of a layer MnO_2 , and E_{*OH} , E_{*O} , and E_{*OOH} are the energy of the $*O$, $*OH$, and $*OOH$ adsorption on a layer MnO_2 , respectively. The E_{H_2} and E_{H_2O} are the energy of H_2O and H_2 molecules in the gas phase. Moreover, the zero-point energy (ZPE) and entropy correction were also considered to transform adsorption DFT energies into adsorption Gibbs free energies through the formula as follows:

$$\Delta G = \Delta E^{DFT} + \Delta ZPE - T\Delta S \quad (S8)$$

where ΔE^{DFT} is the adsorption energy obtained from DFT calculation, ΔZPE is zero-point energy change, the T is the temperature and ΔS is the entropy change. The ZPE and S values together with solvent corrections were acquired from references 11-13 as shown in Table S1.

To study OER/ORR reactions, a computational standard hydrogen electrode (CHE) model proposed by Nørskov et al. [11] was employed to calculate the free-energy diagrams of OER and ORR on different layer MnO_2 . In CHE model, the chemical potential of a proton/electron ($H^+ + e^-$) can be reference with a half of the chemical potential of a gaseous H_2 . The free energies change (ΔG) for each reaction step is given by the following equation:

$$\Delta G = \Delta E + \Delta ZPE - T\Delta S + \Delta G_U + \Delta G_{pH} \quad (S9)$$

in which, ΔE is the reaction energy of reactant and product molecules adsorbed on a catalytic surface. ΔG_U stands for the effect of an external bias which is shifted by $-eU$ where e is the transferred charge and U is the applied bias. ΔG_{pH} is the H^+ free energy correction by the concentration dependence of the entropy: $\Delta G_{pH} = -k_B T \ln[H^+] = k_B T \ln 10 \times pH$.

According to equation S8 and S9, the free energy change of four reaction steps is given by the expression with the adsorption free energies of OER/ORR intermediates as follows:

$$\Delta G1 = \Delta G_{*OH} - eU + k_B T \ln 10 \times pH \quad (S10)$$

$$\Delta G2 = \Delta G_{*O} - \Delta G_{*OH} - eU + k_B T \ln 10 \times pH \quad (S11)$$

$$\Delta G3 = \Delta G_{*OOH} - \Delta G_{*O} - eU + k_B T \ln 10 \times pH \quad (S12)$$

$$\Delta G4 = 4.92 - \Delta G_{*OOH} - eU + k_B T \ln 10 \times pH \quad (S13)$$

In this calculation, the standard condition where $pH = 0$ and $T = 298.15$ K and $U = 0$ are considered. In equation S13, we used the term 4.92 eV which is the free energy of the water splitting process due to the difficulty to produce accurate energy of O_2 molecule with the employed method.

Base on the developed a method by Nørskov et al.⁸ the overpotential of OER and ORR are calculated as follow:

$$\eta^{\text{OER}} = \max(\Delta G_1, \Delta G_2, \Delta G_3, \Delta G_4/e) - 1.23 \text{ V} \quad (\text{S14})$$

$$\eta^{\text{ORR}} = 1.23 - \min(\Delta G_1, \Delta G_2, \Delta G_3, \Delta G_4/e) \text{ V} \quad (\text{S15})$$

Table S1. Zero-point energy (ZPE) corrections and entropic contributions (TS) along with solvent corrections (G_{solv}) to free energies of gas phase and adsorbed intermediates species taken from ref 11-13 (all energies are in eV).

Species	ZPE	TS	G_{solv}
H ₂ O _(l)	0.56	0.67	0.00
H ₂ _(g)	0.27	0.41	0.00
*O	0.07	0.00	0.00
*OH	0.30	0.00	-0.30
*OOH	0.39	0.00	-0.30

Table S2. Free energies of the OER and ORR adsorbates, *OH, *O, and *OOH in eV unit and overpotentials of OER and ORR in V unit of the layer MnO₂ catalysts.

Cat.	ΔG_{*OH}	ΔG_{*O}	ΔG_{*OOH}	ΔG_1	ΔG_2	ΔG_3	ΔG_4	η^{OER}	η^{ORR}
LiMnO ₂	2.87	3.39	4.38	2.87	0.52	0.99	0.54	1.64	0.71
NaMnO ₂	2.93	3.82	4.75	2.93	0.89	0.93	0.17	1.70	1.06
KMnO ₂	3.02	3.81	4.82	3.02	0.79	1.01	0.10	1.79	1.13
RbMnO ₂	3.06	3.62	4.84	3.06	0.56	1.22	0.08	1.83	1.15
CsMnO ₂	3.07	3.83	4.83	3.07	0.76	1.00	0.09	1.84	1.14

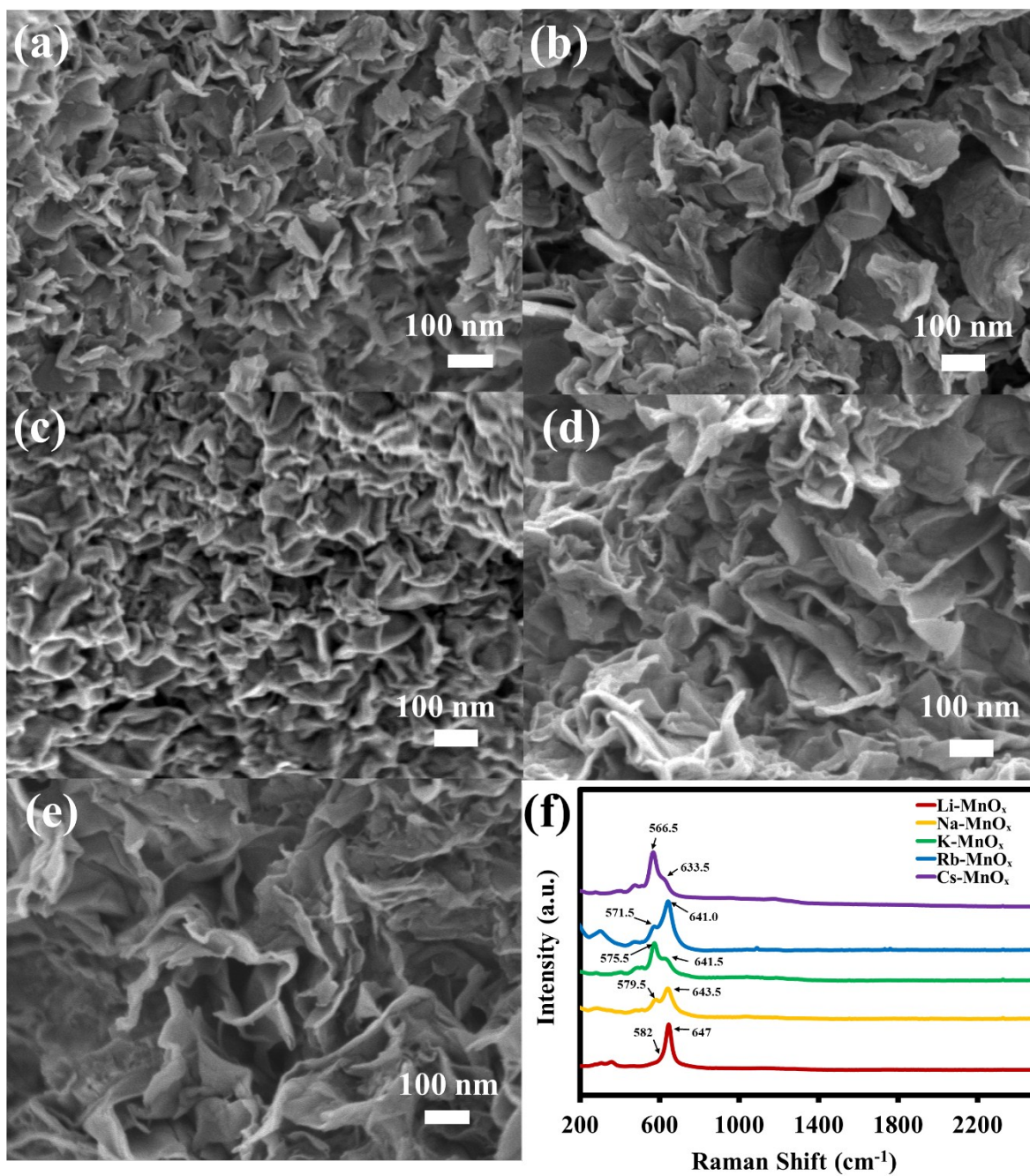


Figure S1. FESEM images of birnessite-type layered manganese oxides; (a) Li-MnO_x, (b) Na-MnO_x, (c) K-MnO_x, (d) Rb-MnO_x, (e) Cs-MnO_x along with (f) Raman spectra of the layered manganese oxides.

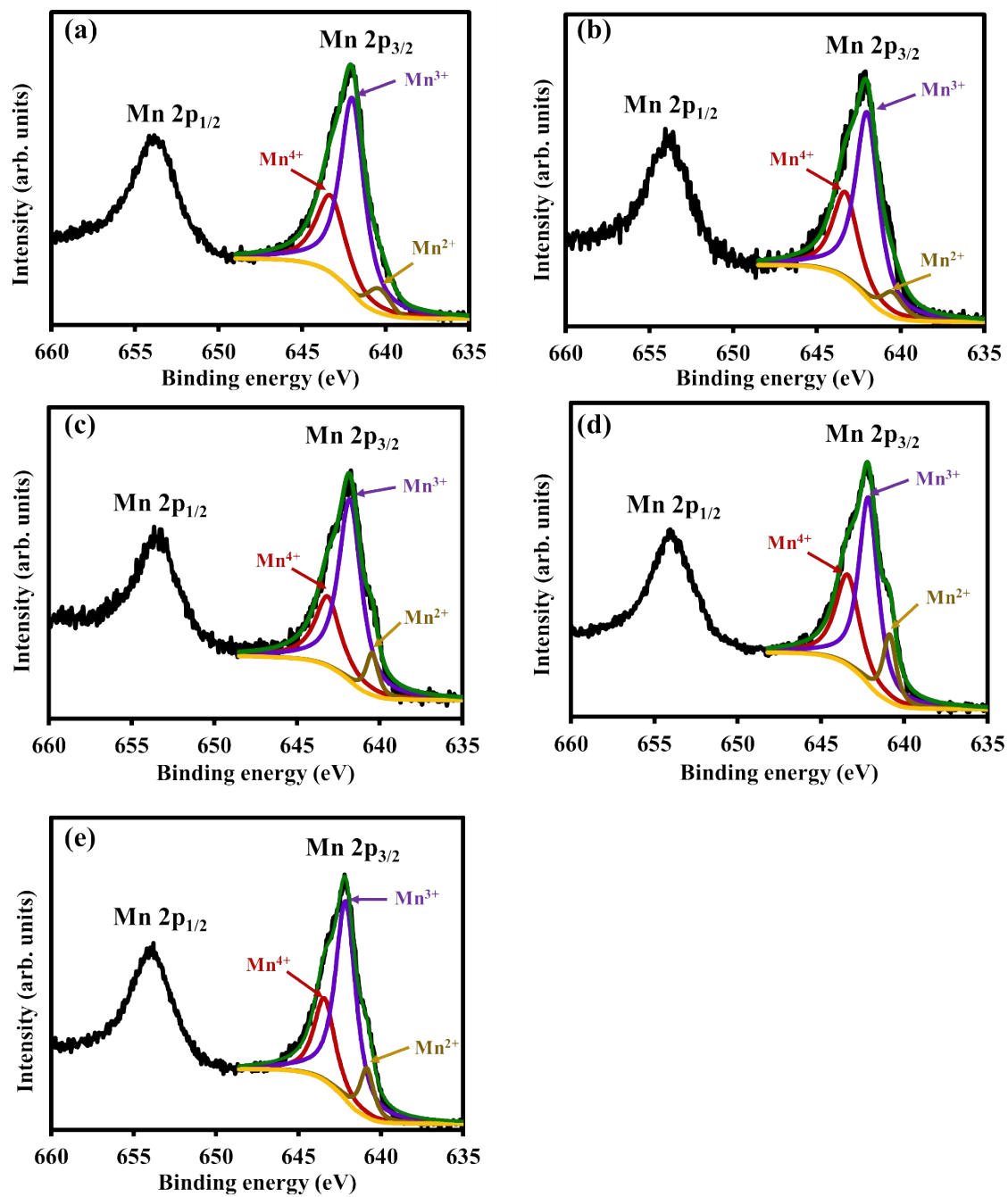


Figure S2. Mn 2p XPS spectra of (a) Li-MnO_x, (b) Na-MnO_x, (c) K-MnO_x, (d) Rb-MnO_x, and (e) Cs-MnO_x.

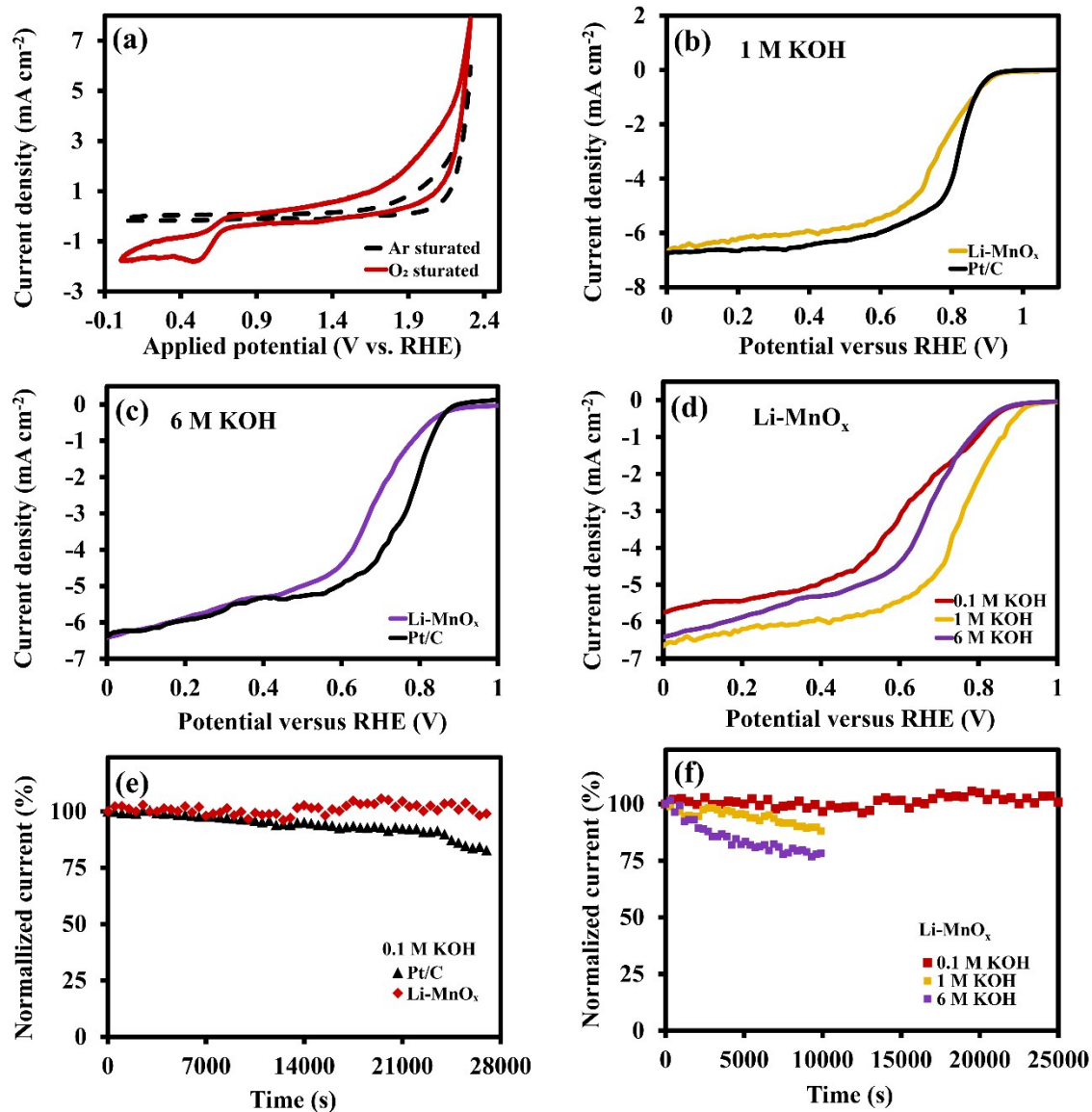


Figure S3. Electrochemical performance and stability of the layered manganese oxides; (a) cyclic voltammograms of a Li-MnO_x in O₂ (red line) and Ar (black line) saturated 0.1 M KOH solution at a scan rate of 100 mV s⁻¹, (b) LSV curves of the Li-MnO_x versus a commercial Pt/C loading on CFP (0.3 mg cm⁻²) in 1 M and (c) 6 M KOH solutions at a scan rate of 10 mV s⁻¹, (d) the comparison of the ORR catalytic activity of the Li-MnO_x in various OH⁻ concentration at a scan rate of 10 mV s⁻¹, (e) stability of the Li-MnO_x versus Pt/C in O₂-saturated 0.1 M KOH solution at a constant potential of 0.7 V versus RHE, and (f) the stability of the Li-MnO_x in different concentration of OH⁻ ions at a constant potential of 0.7 V versus RHE.

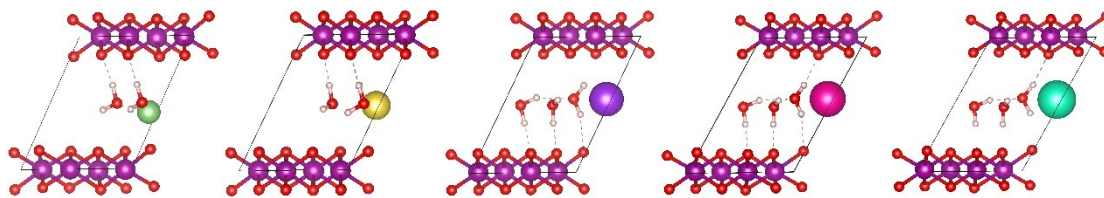


Figure S4. Unit cell of the MnO₂ layer catalysts. The red, white, green, yellow, light purple, pink, light green and purple represent the O, H, Li, Na, K, Rb, Cs and Mn atoms, respectively.

References

1. Q. Feng, K. Yanagisawa and N. Yamasaki, *J. Ceram. Soc. Jpn.*, 1996, **104**, 897-899.
2. Q. Feng, K. Yanagisawa and N. Yamasaki, *J. Mater. Sci. Lett.*, 1997, **16**, 110-112.
3. Q. Feng, E.-H. Sun, K. Yanagisawa and N. Yamasaki, *J. Ceram. Soc. Jpn.*, 1997, **105**, 564-568.
4. J. Zhang, Z. Zhao, Z. Xia and L. Dai, *Nat. Nanotechnol.*, 2015, **10**, 444.
5. X. Min, Y. Chen and M. W. Kanan, *Phys. Chem. Chem. Phys.*, 2014, **16**, 13601-13604.
6. Z. Luo, S. Lim, Z. Tian, J. Shang, L. Lai, B. MacDonald, C. Fu, Z. Shen, T. Yu and J. Lin, *J. Mater. Chem.*, 2011, **21**, 8038-8044.
7. P. Iamprasertkun, C. Tangarnjanavalukul, A. Krittayavathananon, J. Khuntilo, N. Chanlek, P. Kidkhunthod and M. Sawangphruk, *Electrochimica Acta*, 2017, **249**, 26-32.
8. P. Iamprasertkun, A. Krittayavathananon, A. Seubsai, N. Chanlek, P. Kidkhunthod, W. Sangthong, S. Maensiri, R. Yimmirun, S. Nilmoung, P. Pannopard, S. Ittisanronnachai, K. Kongpatpanich, J. Limtrakul and M. Sawangphruk, *Sci. Rep.*, 2016, **6**, 37560.
9. A. Krittayavathananon, T. Pettong, P. Kidkhunthod and M. Sawangphruk, *Electrochimica Acta*, 2017, **258**, 1008-1015.
10. T. Pettong, P. Iamprasertkun, A. Krittayavathananon, P. Sukha, P. Sirisinudomkit, A. Seubsai, M. Chareonpanich, P. Kongkachuichay, J. Limtrakul and M. Sawangphruk, *ACS Appl. Mater. Interfaces*, 2016, **8**, 34045-34053.
11. S. Daengsakul, P. Kidkhunthod, O. Soisang, T. Kuenoon, A. Bootchanont and S. Maensiri, *Microelectron Eng*, 2015, **146**, 38-42.
12. J.-K. Chang, M.-T. Lee, W.-T. Tsai, M.-J. Deng and I. W. Sun, *Chem. Mater.*, 2009, **21**, 2688-2695.